Cellulose (2018) 25:49–64
https://doi.org/10.1007/s10570-017-1547-8

ORIGINAL PAPER

Comparison and validation of Fourier transform infrared spectroscopic methods for monitoring secondary cell wall cellulose from cotton fibers

Hee Jin Kim · Yongliang Liu · Alfred D. French · Christopher M. Lee · Seong H. Kim

Received: 22 August 2017 / Accepted: 28 October 2017 / Published online: 10 November 2017

Abstract The amount of secondary cell wall (SCW) cellulose in the fiber affects the quality and commercial value of cotton. Accurate assessments of SCW cellulose are essential for improving cotton fibers. Fourier transform infrared (FT-IR) spectroscopy enables distinguishing SCW from other cell wall components in a rapid and non-invasive way. Thus it has been used for monitoring SCW development in model plants. Recently, several FT-IR methods have been proposed for monitoring cotton fiber development. However, they are rarely utilized for assessing SCW cellulose from cotton fiber due to limited validation with various cotton species grown in different conditions. Thus, we compared and validated three FT-IR methods including two previously proposed methods analyzing entire spectra or specific bands as well as a new method analyzing FT-IR spectral regions corresponding to cellulose with various cotton fibers grown in planta and in vitro. Comparisons of the FT-IR methods with reference methods showed that the two FT-IR methods analyzing the entire spectra or cellulose regions by principal component analysis monitored SCW qualitatively, whereas the FT-IR method analyzing specific bands (708, 730, and 800 cm^{-1}) by a simple algorithm allowed the monitoring of SCW cellulose levels quantitatively. The quantitative FT-IR method is a potential substitute for lengthy and laborious chemical assays for monitoring SCW cellulose levels from cotton fibers, and it can be used for a better understanding of cotton fiber SCW development and as a part of the quality assessment tools used to guide choices for improving fiber quality.

Keywords Attenuated total reflection Fourier transform infrared (ATR FT-IR) spectroscopy · Cotton fiber property · Cellulose · Crystallinity · Secondary cell wall (SCW)

Electronic supplementary material The online version of this article (https://doi.org/10.1007/s10570-017-1547-8) contains supplementary material, which is available to authorized users.

H. J. Kim (✉)
Cotton Fiber Bioscience Research Unit, Southern Regional Research Center, USDA-ARS, 1100 Robert E. Lee Blvd., New Orleans, LA 70124, USA
e-mail: heejin.kim@ars.usda.gov

Y. Liu · A. D. French
Cotton Structure and Quality Research Unit, Southern Regional Research Center, USDA-ARS, 1100 Robert E. Lee Blvd., New Orleans, LA 70124, USA

C. M. Lee · S. H. Kim
Department of Chemical Engineering and Materials Research Institute, Pennsylvania State University, University Park, PA 16802, USA

C. M. Lee · S. H. Kim
Center for Lignocellulose Structure and Formation, Pennsylvania State University, University Park, PA 16802, USA

Introduction

Cotton (*Gossypium* sp.) is the most important natural fiber in the world (Wakelyn et al. 2010). Its fibers are mainly composed of secondary cell wall (SCW) cellulose that determines fiber properties and quality (Hsieh 1999; Kim et al. 2014, 2017; Meinert and Delmer 1977). For phenotyping cotton fibers and interpreting cotton genomics information, the cotton research community has used two automated instruments, high-volume instrument (HVI) and advanced fiber information system (AFIS). These systems were originally designed for determining the market value of cotton fibers or for predicting spinning performance and yarn quality. Micronaire (MIC) and maturity ratio (MR) values indirectly measured by the automated instruments are used for phenotyping SCW of cotton fibers and interpreting genetic and genomic data. However, they are not sensitive enough to detect minor differences in SCW levels from cotton fibers (Kim et al. 2017; Paudel et al. 2013; Rodgers et al. 2013).

To identify cotton genes regulating fiber properties, cotton scientists have been using comparative genomic analyses that compare the transcriptomic profiles or gene expression patterns of two developing cotton fibers differing in fiber properties or quality (Kim 2015). When these genomic data were interpreted with the fiber phenotypic data that were mostly measured by the HVI and AFIS instruments, common genes were identified for regulating two different fiber development processes, SCW development (Wang et al. 2014) and fiber elongation (Fang et al. 2014). Thus, methods for phenotyping SCW cellulose more reliable and sensitive than HVI and AFIS are needed to improve gene discovery and fiber quality through cotton genetic and genomic studies that are rapidly advancing with emerging techniques.

Several methods including Updegraff cellulose content analysis (Updegraff 1969) and X-ray diffraction (XRD) (Nam et al. 2016), and image analysis microscopy of cross-sectioned fibers (Gordon and Rodgers 2017) can be used for monitoring SCW cellulose from cotton fibers. However, those methods are unfavorable to cotton geneticists and breeders due to their lengthy and complicated processes (Rodgers et al. 2013). An indirect method, Cottonscope is used as a supplement to the direct image analysis (Brims and Hwang 2010). It rapidly estimates the degree of SCW development by measuring birefringence intensity from developing cotton fibers (Long et al. 2010) despite the results can be affected by the levels of physiological sugars causing stickiness in developing fibers (Kim et al. 2014).

In contrast, Fourier transform infrared (FT-IR) spectroscopy has been extensively used by plant biologists to identify SCW in a rapid and non-invasive way from model plants like Arabidopsis and corn (McCann et al. 1992). To analyze large data sets of FT-IR spectra effectively, a mathematical technique known as principal component analysis (PCA) is frequently used (Abidi et al. 2010a, 2014; Kemsley 1998). The first principal component (PC1) score was observed to increase with cotton fiber DPA consistently and significantly (Abidi et al. 2010a, 2014; Liu and Kim 2015), while the second PC (PC2) score could provide complementary information to the PC1 score. Thus, the FT-IR spectroscopy with the PCA method was successfully used for screening for mutants that were SCW deficient, studying SCW formation, identifying novel genes involved in SCW cellulose biosynthesis, and determining roles of plant polysaccharide compositions in cell walls (Brown 2005; Chen et al. 1998; McCann et al. 2001; Mouille et al. 2003; Vorwerk et al. 2004).

FT-IR spectroscopy and PCA method have been introduced to study cotton fiber. Abidi and his colleagues used the entire FT-IR spectra (600–3800 cm^{-1}) for PCA analysis to monitor cotton fiber development by evaluating fiber wall composition (Abidi et al. 2008), SCW (Abidi et al. 2010a), and sugar composition (Abidi et al. 2010b). Later, there were several attempts to extract cotton fiber SCW information from a few specific FT-IR bands with new algorithms. The intensity ratios of three FT-IR bands such as 956, 1032, and 1500 cm^{-1} (Liu et al. 2011), 708, 730, and 800 cm^{-1} (Liu et al. 2012a), and 1236, 1315, or 1800 cm^{-1} (Liu and Kim 2015) were proposed to correlate with fiber maturity, crystallinity, and fiber development, respectively. The integrated intensities of two FT-IR bands, 667 and 897 cm^{-1} were also proposed to correlate with the percentage crystallinity (Abidi et al. 2014; Abidi and Manike 2017). The FT-IR methods using either entire spectra or a few specific bands were tested with limited numbers of upland cotton varieties, but were not validated with various cotton species and lines grown in different conditions that cotton biologists frequently

use for their studies. Therefore, the FT-IR methods have been rarely utilized by cotton geneticists and breeders. Interestingly, the FT-IR spectral regions corresponding to cellulosic components have not been tested unlike the entire FT-IR spectra and specific bands.

In this present work, we determined which FT-IR methods can quantitatively determine SCW cellulose development for various cotton fibers including developing and developed fibers from different cotton species grown in planta or in vitro. In addition to the two known FT-IR methods analyzing entire spectra (600–3800 cm^{-1}) or specific bands (708, 730, and 800 cm^{-1}), we analyzed the various cotton fibers with the FT-IR spectral regions corresponding to cellulosic components (700–760, 950–1020, 1100–1200, 1260–1340, and 3200–3400 cm^{-1}). Comparisons of the SCW cellulose levels determined by the FT-IR methods with the reference methods including Updegraff, XRD, and gene expression assays showed strengths and weakness of each FT-IR method. Among the three FT-IR methods, a FT-IR method with the specific FT-IR bands allowed quantifying cotton fiber SCW cellulose, whereas the two other methods could only distinguish SCW from PCW qualitatively.

Experimental

Materials and sample preparation

Developing cotton fibers were harvested from *Gossypium hirsutum*, Texas marker-1 (TM-1, PI 607172) that is a standard polyploid upland cotton variety for genetic and genomic research (Kohel et al. 1970; Zhang et al. 2015) and *G. arboreum* Shixiya1 (SXY1) that is a standard diploid cotton used for genome sequencing (Li et al. 2014). Cotton flowers grown in the field of USDA-ARS in New Orleans, LA were tagged at the day of anthesis (DOA) and developing fibers from 10 to 30 cotton bolls were harvested from multiple cotton plants for two biological replications at various developmental stages in 2011 (10, 17, 24, 28, 33, and 37 days post anthesis, DPA) and 2015 (12, 23, and 30 DPA). The developing fibers were manually cut from the seeds and dried at 40 °C. Cotton bolls were fully developed and opened at 42–44 DPA. The fully dried and developed fibers were harvested and ginned with a laboratory roller gin. The soil type in New Orleans is Aquent dredged over alluvium and is elevated to provide adequate drainage.

Cotton ovule culture

Unfertilized ovules at flowering day (DOA) from the upland variety TM-1 were used for cotton ovule culture. The ovules were incubated on Beasley and Ting (BT) medium with two different phytohormone conditions (Beasley and Ting 1974). One contained a natural auxin, indole-3-acetic acid (IAA, 5.0 μM) with 0.5 μM gibberellic acid (GA_3) and the other had a synthetic auxin, 1-naphthaleneacetic acid (NAA, 5.0 μM) with 0.5 μM GA_3. Cotton ovules were cultured in the darkness at 30 °C in a 5% CO_2 atmosphere. The cultured ovules at different developmental stages (13, 17, 24, and 27 DPA) were harvested and manually cut from the seeds. The collected fibers were frozen immediately with liquid nitrogen for RNA extraction or dried in a 40 °C incubator for physical property analyses.

RNA extraction and gene expression assay by RT-qPCR

Total RNA was extracted from developing fibers at 13, 17, 24 and 27 DPA using the Sigma Spectrum™ Plant Total RNA Kit (Sigma-Aldrich, St. Louis, MO) with DNase I digestion according to the manufacturer's protocol. The quality and quantity of total RNA were determined using a NanoDrop 2000 spectrophotometer (NanoDrop Technologies Inc., Wilmington, DE). Two biological replications were used for RNA extractions. The experimental procedures and data analysis related to RT-qPCR were performed according to the Minimum Information for Publication of Quantitative Real-Time PCR Experiments guidelines. Abundances of *GhCesA2* transcripts encoding cellulose synthase catalytic subunit were compared by RT-qPCR analyses. The detailed description of cDNA preparation, qPCR, and calculations were previously reported (Kim et al. 2013a). Specific primer pairs were designed from the *GhCesA2* encoding cellulose synthase catalytic subunit (Table 1). The endogenous reference genes, *18S rRNA* and *α-tubulin 4,* were used for normalizing the transcript levels. Three biological replications and three technical replications for each time-point were used for RT-qPCR.

Table 1 Primer sequences for quantitative RT-PCR

Gene ID	Forward primer (5′–3′)	Reverse primer (5′–3′)
GhCesA2	TGTTGATTTGCTGTGATTCTAAAAGGGATT	GAAATTAAATTGAACCAACAAAATCATAGG
18S rRNA	CGTCCCTGCCCTTTGTACA	AACACTTCACCGGACCATTCA
α-tubulin 4	GATCTCGCTGCCCTGGAA	ACCAGACTCAGCGCCAACTT

Cellulose content measurement

Cellulose contents of developing fibers at various DPAs and fully developed fibers were measured by the method described by Updegraff (1969) with minor modifications. Dried fiber samples were cut into small pieces. Ten milligrams of the fibers were placed to 5 mL of reacti-vials. Non-cellulosic materials in fibers were hydrolyzed with the Updegraff reagent (73% acetic acid, 9% nitric acid, and 18% water). The remaining cellulose was hydrolyzed with 67% sulfuric acid (v/v) and measured by a colorimetric assay with anthrone. Avicel PH-101 (FMC, Rockland, ME) was used as a cellulose standard. A_{650} from the samples and standards was measured by a plate reader (ThermoMax, Molecular Devices, Sunnyvale, CA). The average cellulose content for fibers was obtained from two biological and three technical replications.

ATR FT-IR spectral collection and data analysis

All spectra were collected with an FTS 3000MX FTIR spectrometer (Varian Instruments, Randolph, MA) equipped with a ceramic source, KBr beam splitter, and deuterated triglycine sulfate (DTGS) detector as previously described in Liu and Kim (2015). The ATR sampling device utilized a DuraSamplIR single-pass diamond-coated internal reflection accessory (Smiths Detection, Danbury, CT) and consistent contact pressure was applied by way of a stainless steel rod and an electronic load display. At least six measurements at different locations for individual samples were collected over the range of 600–4000 cm^{-1} at 4 cm^{-1} and 16 co-added scans. All spectra were given in absorbance units and no ATR correction was applied. Following the import to GRAMS IQ application in Grams/AI (Version 9.1, Thermo Fisher Scientific, Waltham, MA), the spectra were smoothed with a Savitzky–Golay function (polynomial = 2 and points = 11). Then, the spectral set was loaded into Microsoft Excel 2000 to assess CI_{IR} values from IR measurement by using a previously proposed algorithm analysis (Liu et al. 2011, 2012a). Principal component analysis (PCA) calculations for IR spectra were performed in the 600–3800 cm^{-1} IR region with mean centering (MC) and Savitzky–Golay first-derivative (2 degrees and 13 points) spectral pretreatment and also with leave-one-out cross-validation method, after these spectra were normalized by dividing the intensity of individual band in the 600–3800 cm^{-1} region with the average intensity in this 600–3800 cm^{-1} region.

X-ray diffraction (XRD)

XRD experiments were performed with a PANalytical Empyrean diffractometer (PANalytical, Netherlands), equipped with a Cu X-ray source ($\lambda = 1.5404$ Å), and operated at 45 kV and 40 mA. The instrumental profile was calibrated with LaB_6 (NIST 660a). Fully dried cotton samples were ground in a Wiley mill to 20 mesh, hand pressed into a pellet, and placed on a quartz zero-background holder before analysis. Scans were measured in the 2θ range of 8°–45° in 0.05° steps. The fitting procedures using a peak deconvolution method for cellulose crystallinity index (CI_{XRD}) in developing cotton fibers were described earlier (Lee et al. 2015b). The diffraction data were also analyzed by Rietveld method that is incorporated in the MAUD software (Lutterotti 2010). The refinements typically included 11 variables, including scale factor, quadratic background, unit cell a and gamma, crystallite size, amorphous particle size, preferred orientation along (00l) axis for both phases, and amount of phase 1, amount of phase 2. The detailed Rietveld refinement information of the developing fibers was previously described in Kim et al. (2017).

Statistical analyses

Statistical analyses and construction of graphs were performed using *t* test, two-way ANOVA and Prism version 5 software (Graph-Pad Software, Inc., San Diego, CA). The *p*-value cutoff for significance was 0.05.

Results and discussion

Determination of cotton fiber SCW cellulose development by a chemical reference assay

Cotton fibers elongated during PCW biosynthesis stage after they were differentiated from ovule epidermis of upland cotton variety TM-1 around the day of anthesis (Fig. 1a). Cellulose contents of developing fibers were determined by the Updegraff method (Updegraff 1969), which is a destructive chemical analysis requiring lengthy and laborious processes, but also generally considered as a reference method for determining SCW development in upland cotton fibers (Meinert and Delmer 1977). Developing fibers at PCW stage (10 DPA) consisted of low cellulose content (6.7%) while they were actively elongated (Fig. 1b and Table 2). At transition (17 DPA) from PCW to SCW biosynthesis stage, the cellulose content of developing cotton fibers increased dramatically to 32.8%. During the active SCW biosynthesis stage (20–37 DPA), the cellulose contents continued increasing and reached 90.4% at 37 DPA. Cotton bolls became fully developed and opened approximately 42–44 DPA. The fully developed fibers were harvested at 44 DPA after they were dehydrated in the field. They were composed of nearly pure cellulose. The TM-1 fiber development pattern was consistent with the developmental pattern that was previously reported by our group and others (Haigler 2010; Kim 2015; Kim and Triplett 2001; Meinert and Delmer 1977).

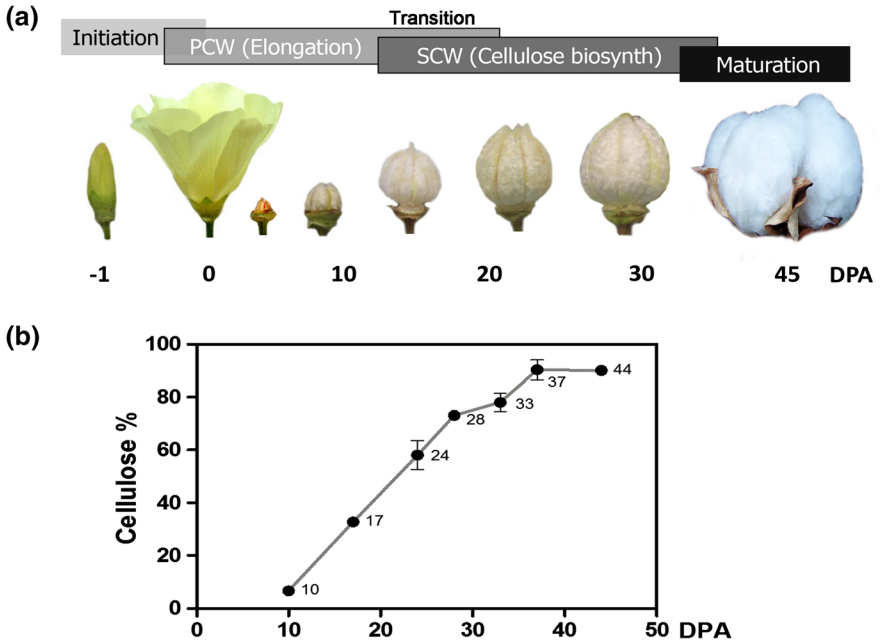

Fig. 1 Cotton fiber development and cellulose biosynthesis. **a** Development of an upland cotton TM-1 variety. Four major fiber developmental stages are classified based on the physical properties described in Kim (2015). The ovary walls were removed from developing cotton bolls to show the cotton fiber growth inside the bolls. Fully developed bolls were naturally opened at 42–44 DPA and developed fibers were harvested at 44 DPA. PCW, primary cell wall stage for fiber elongation; SCW, secondary cell wall stage for cellulose biosynthesis; DPA, days post anthesis. **b** Cellulose content was determined from developing TM-1 fibers (10–44 DPA) by the method described by Updegraff (1969)

Table 2 Fiber properties of developing *G. hirsutum* TM-1 fibers measured by Updegraff assay and ATR FT-IR spectroscopy

DPA	Updegraff assay		ATR FT-IR method			
	Cellulose (%)		PC1 from full IR spectra (600–3800 cm^{-1})		CI_{IR} % from the 3 IR bands (708, 730 and 800 cm^{-1})	
	M	SD	M	SD	M	SD
10	6.7	0.2	− 0.473	0.037	11.9	0.1
17	32.8	1.7	− 0.099	0.059	32.7	3.8
24	58.0	5.5	0.106	0.001	48.2	3.2
28	73.1	0.7	0.096	0.029	49.0	4.0
33	78.0	3.5	0.048	0.027	61.4	6.9
37	90.4	3.7	0.067	0.026	61.6	7.7
44	90.1	1.4	0.133	0.093	75.1	10.5

Average values (M) were calculated from two biological replicates that were harvested at various developmental stages. Three and six technical replicates were used for the Updegraff assay and ATR FT-IR method, respectively. CI_{IR} %, crystallinity percentage determined by a FT-IR algorithm described in Liu et al. (2012a)

Determination of FT-IR spectral regions corresponding to cellulosic components during cotton fiber development

ATR FT-IR spectra (600–3800 cm^{-1}) were obtained from developing fibers at 10, 17, 24, 28, 33, and 37 DPA and developed fibers at 44 DPA (Fig. 2a). The characteristic bands of these developing fibers were assigned in Supplementary Table S1 according to the previously published reports (Abidi et al. 2010a, 2014; Kim et al. 2013b; Liu and Kim 2015). As DPA increased, the intensities of the bands at 1740, 1620, 1545, 1455, 1405, and 1236 cm^{-1} as well as those below 850 cm^{-1} decrease, whereas those at 1425, 1365, 1335, 1315, 1200, 1158, 1104, 1055, and 1028 cm^{-1} as well as those in the 895 cm^{-1} region increase. These intensity distinctions suggest chemical, compositional, and structural changes during cotton fiber cellulose development, and subsequently these unique bands have proved to be effective in monitoring the increasing dominance of SCW.

The PCAs were performed with entire spectra including all vibration modes from non-cellulosic components as well as cellulose. The principal component (PC1) loadings feature negative and positive peaks, with large positive (or negative) loadings contributing largely to positive (or negative) PC1 scores. In the PC1 loading plot, the peaks pointing downwards are the ones dominant in PCW (water, hemicellulose, cuticles, proteins, and pectin), whereas the peaks pointing upwards are the component dominant in SCW that are mostly composed of cellulose in cotton fibers. Several negative peaks were found from water peaks at 1640 and 3100–3600 cm^{-1}, protein peaks at 1520–1650 cm^{-1}, pectin peaks at 1740 cm^{-1}, and long-chain alkyl hydrocarbon peaks at 2850 and 2926 cm^{-1} (Fig. 2b and Table S1). Based on the previous FT-IR work by Abidi et al. (2014) and Lee et al. (2015), the PC scores in the gray shaded regions in Fig. 2b have strong contributions from non-cellulosic components. Thus, the five blue regions [I (700–760 cm^{-1}), II (950–1020 cm^{-1}), III (1100–1200 cm^{-1}), IV (1260–1340 cm^{-1}), and V (3200–3400 cm^{-1})] with positive PC scores in Fig. 2b can be attributed to cellulose.

Estimation of SCW development with entire FT-IR spectra and PCA approach

All ATR FT-IR spectra (600–3800 cm^{-1}) obtained from developing TM-1 fibers were analyzed by the conventional PCA method. The PC1 score dramatically increased from 10 to 17 DPA due to the transition from PCW to SCW stage, reached the maximal value at 24 DPA, and plateaued from 24 to 44 DPA (Fig. 3a and Table 2).

Large negative PC1 score at 10 DPA fibers indicates the existence of non-cellulosic components (water, proteins, pectins, and hydrocarbon in the cuticle) in PCW. Positive PC1 scores result from the existence of the SCW cellulose in developing and

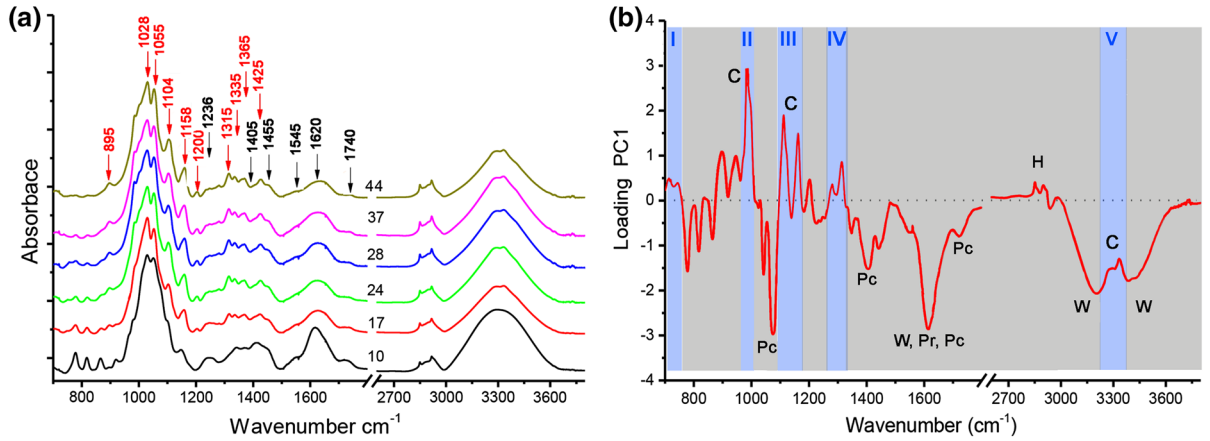

Fig. 2 FT-IR analyses of cotton fibers. **a** Comparative ATR FT-IR spectra of developing fibers from 10 to 37 DPA and fully developed fibers at 44 DPA from an upland cotton variety TM-1. During fiber development, the wavenumbers with increasing and decreasing intensities were marked with red and black arrows, respectively. **b** PCA of entire data set and loading plot of principal component 1, PC-1 (93% explained variance) representing the predominant spectral elements. The letters C, H, Pc, Pr, and W indicate cellulose, hydrocarbon, pectin, protein, and water components, respectively. The dotted line represents zero PC1 loading. In the regions shaded with gray, PCl scores were mostly contributed by non-cellulosic components. Five regions (I–V) contributed by cellulosic components were identified and highlighted with blue

developed fibers. The pattern of increasing PC1 scores from 10 to 24 DPA was compared with that of cellulose content (Fig. 3b). There was a positive correlation ($r = 0.896$; $R^2 = 0.803$) between the cellulose content and PC1 scores from 10 to 44 DPA. However, the PC1 scores from 24 to 44 DPA showed no significant correlations ($r = -0.022$, $R^2 = 0.0005$, $p = 0.972$) with the cellulose contents during the SCW stage. The results confirmed that the PC1 scores determined by the PCA method from the entire FT-IR spectra (600–3800 cm^{-1}) can distinguish the transition from PCW to SCW biosynthesis during cotton fiber development. However, the PCA scores were not sensitive enough to show the progress of fiber development during SCW biosynthesis stage (24–44 DPA), unlike the Updegraff cellulose assay showing the progress of SCW biosynthesis (Figs. 1, 3).

Estimation of SCW development with FT-IR spectral regions corresponding to cellulosic components and PCA approach

The PCA with entire spectra from 10 to 44 DPA fibers proved the difference between PCW and SCW but failed to quantitatively measure the degree of SCW cellulose from 24 to 44 DPA fibers (Fig. 3b). Thus, we re-ran PCA for the four IR regions [I (700–760 cm^{-1}), III (1100–1200 cm^{-1}), IV (1260–1340 cm^{-1}), and V (3200–3400 cm^{-1})] that specifically corresponded to cellulose (Fig. 2b). The patterns (Fig. 4a) of PC1 scores performed with the cellulose IR regions showed striking similarities to those (Fig. 3a) performed with entire IR spectra.

The PC1 score increased significantly from 10 to 17 DPA due to the transition from PCW development to SCW development, reached the maximum value at 24 DPA, and plateaued from 24 to 44 DPA (Fig. 4a). The correlation ($r = 0.899$, $R^2 = 0.807$) between PC1 scores and cellulose content obtained from the cellulose IR regions (Fig. 4b) was also almost identical to that obtained from the entire IR spectra (Fig. 3b). The PC1 scores from 24 to 44 DPA showed no significant correlations ($r = 0.160$, $R^2 = 0.026$, $p = 0.797$) with cellulose content during the SCW stage.

Since it was originally expected the method with the FT-IR spectral regions specific for cellulose to be much better for monitoring SCW cellulose development than that with the entire FT-IR spectra of cotton fibers, it was surprising that the PC1 scores determined with the cellulose-characteristic regions provided only marginally better correlations (p and R^2 values) than those based on the entire IR spectra. Neither the combined cellulose regions nor individual cellulose IR regions [I (700–760 cm^{-1}), III (1100–1200 cm^{-1}), or IV (1260–1340 cm^{-1})] were able to quantify the SCW biosynthesis (Supplementary Fig. S1). Based on the

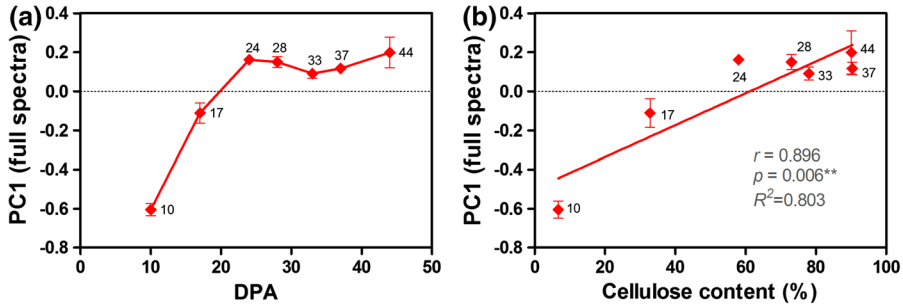

Fig. 3 Comparisons between cellulose contents (%) and PC1 scores determined from FT-IR full spectra (600–3800 cm^{-1}) of developing cotton fibers. **a** PC 1 scores were calculated from FT-IR spectra of developing fibers at various DPA. **b** Correlation between cellulose content and PC1 scores from developing fibers. The correlation coefficient values (r) were obtained by Pearson's method, and R^2 values were determined by GraphPad Prisim software. Statistical significance was shown at the probability (p) levels value under 0.05*, 0.01**, and 0.001***

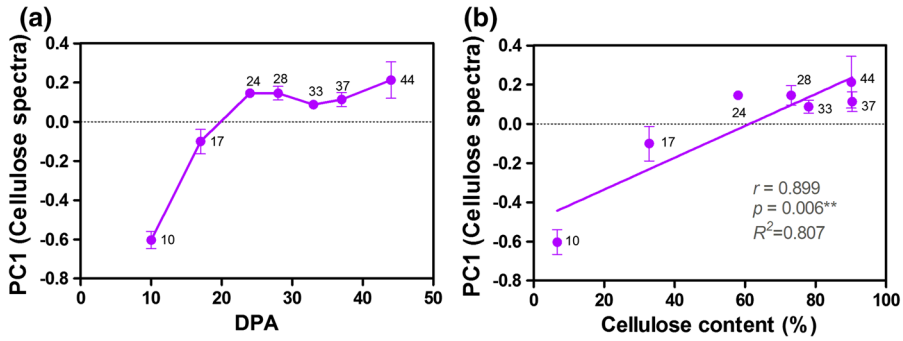

Fig. 4 Comparisons between cellulose contents (%) and PC1 scores determined from the cellulose FT-IR spectra of developing cotton fibers. **a** PC 1 scores were calculated from four cellulose FT-IR spectral regions [I (700–760 cm^{-1}), III (1100–1200 cm^{-1}), IV (1260–1340 cm^{-1}), and V (3200–3400 cm^{-1})] of developing fibers. **b** Correlation between cellulose content and PC1 scores corresponding to cellulose from developing fibers. The correlation coefficient values (r) were obtained by Pearson's method, and R^2 values were determined by GraphPad Prisim software. Statistical significance was shown at the probability (p) levels value under 0.05*, 0.01**, and 0.001***

PCA analyses in Figs. 3, 4 and S1, we concluded that the PCA method is useful to distinguish between PCW and SCW but fails to show the progress of fiber development during SCW biosynthesis stage.

Estimation of SCW development with FT-IR bands and a three band ratio algorithm

We analyzed the FT-IR bands at 708, 730, and 800 cm^{-1} using a simple three band ratio algorithm to estimate crystallinity index (CI_{IR}) values from cotton fiber FT-IR spectra (Liu et al. 2012a). This method compares the relative intensities of a cellulose-characteristic band and an internal reference band:

$$R_2 = (I_{708} - I_{800})/(I_{730} - I_{800})$$

where I is the absorbance at the specific wavenumbers (Liu et al. 2011). The 708 cm^{-1} band is characteristic to crystalline cellulose I_β and the 730 cm^{-1} band is attributed to cellulose I_α or amorphous cellulose (Imai and Sugiyama 1998; Liu et al. 2012a; Sassi et al. 2000; Yamamoto et al. 1996). The intensity at 800 cm^{-1} is used as a common background for normalization. For a data set of 402 fibers, Liu et al. (2012a) assigned the most immature and mature fibers the CI_{IR} values of 0.0 and 100.0%, respectively, then the CI_{IR} values are determined by converting the relative R^2 value for individual fiber sample.

The increasing trend of the CI_{IR} values during entire fiber development from 10 to 44 DPA (Fig. 5a) was similar to that of the cellulose contents (Table 2).

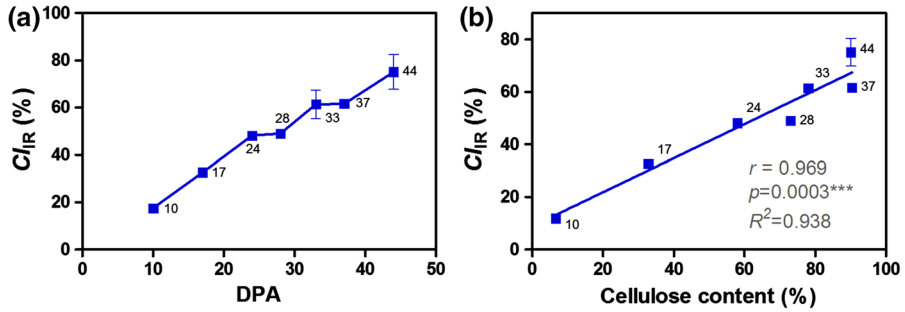

Fig. 5 Correlations of cellulose content with crystallinity index (CI_{IR}). **a** CI_{IR} values were calculated from FT-IR spectra of developing fibers by the TBR algorithm. **b** Correlation between cellulose content and CI_{IR} values from developing fibers (10–44 DPA). The correlation coefficient values (r) were obtained by Pearson's method, and R^2 values were determined by GraphPad Prisim software. Statistical significance was shown at the probability (p) levels value under 0.05*, 0.01**, and 0.001***

There was a significant correlation ($r = 0.969$; $R^2 = 0.938$) between the CI_{IR} values and cellulose contents during entire fiber development (Fig. 5b). During the SCW stage (24–44 DPA), the CI_{IR} values consistently showed significant correlation with the cellulose contents, unlike the PC1 scores that had no correlation in Figs. 3b and 4b. The CI_{IR} standard deviation values in the Table 2 were similar to the variations (1.10–19.49%) that were previously determined from developmental cotton fibers at medium and tip positions of one locule (Liu et al. 2012b).

Thus, we concluded that CI_{IR} values determined from the three FT-IR bands are good indicators of quantitatively measuring the progress of cotton fiber development and good estimators of determining the cellulose quantities during the SCW biosynthesis stage of developing fibers, in addition to those in the PCW and transition stages (10–24 DPA).

Comparison of crystalline cellulose content of cotton fibers measured between XRD and FT-IR methods

The crystallinity of cotton fibers has been widely studied with XRD analysis, and XRD crystallinity index (CI_{XRD}) are often rapidly determined as the relative peak height between crystalline and amorphous materials according to the method that Segal proposed (Segal et al. 1959). However, recent studies showed that there were limits of the Segal crystallinity index (French and Santiago Cintrón 2013; Nam et al. 2016). Driemeier and Calligaris (2011) found that the peak area is more representative of crystalline fraction than the peak height. Thus, we first determined the crystallinity index (CI_{XRD}) values representing the relative amount of crystalline portion in cellulose according to the peak deconvolution method (Kim et al. 2017; Park et al. 2010). Individual crystalline peaks were extracted with curve-fitting process, and CI_{XRD} values of cotton fibers at 17, 24, 37, and 44 DPA were successfully calculated from relative intensities of the fitted diffraction peak and the background component (Table 3 and Fig. 6a). We also analyzed XRD data with another analysis, Rietveld method that is incorporated in the MAUD software (Lutterotti 2010). In the analysis, the cellulose Iβ crystal structure (Nishiyama et al. 2002) was used as a model for the crystalline cellulose I phase, and the cellulose II crystal structure (Langan et al. 2001) was used for the amorphous phase. The 24, 37, and 44 DPA cotton fibers containing high level of SCW cellulose showed excellent fit with the Rietveld model as we previously showed in Kim et al. (2017), whereas the 17 DPA cotton fibers containing high level of PCW component did not fit with the model (Table 3). Therefore, the CI_{XRD} values were only calculated from cotton fibers at 24, 37, and 44 DPA based on the Rietveld method (Table 3). Between the two different XRD analyzing methods, the CI_{XRD} values determined by the Rietveld method were higher than those determined by the deconvolution method.

The crystalline portions of total cellulose were calculated by multiplying either CI_{XRD} or CI_{IR} values with the total cellulose contents determined by the Updegraff method in Table 3. The crystalline portions determined from the XRD by both peak deconvolution and Rietveld methods showed similar increasing patterns with those determined from the FT-IR by

Table 3 Comparison of crystalline cellulose content of cotton fibers measured between XRD and ATR FT-IR methods

DPA	Cellulose content (%)	XRD				ATR FT-IR	
		Deconvolution		Rietveld[a]			
		CI_{XRD} (%)	Crystalline portion (%)	CI_{XRD} (%)	Crystalline portion (%)	CI_{IR} (%)	Crystalline portion (%)
17	33.82 ± 6.10	74	25.03 ± 4.51	–	–	32.70 ± 2.55	11.06 ± 0.86
24	52.55 ± 4.74	66	33.63 ± 3.13	67.2	35.31 ± 3.19	48.20 ± 1.84	25.33 ± 0.97
37	90.36 ± 3.74	68	61.44 ± 2.54	85.1	76.90 ± 3.18	61.60 ± 0.85	55.66 ± 5.15
44	90.12 ± 1.40	64	57.68 ± 0.90	86.8	78.22 ± 1.22	75.10 ± 10.47	67.68 ± 9.44

[a]The CI_{XRD} values determined by the Rietveld method had an excellent fit with other parameters of 24, 37, and 44 DPA fibers, but not with 17 DPA

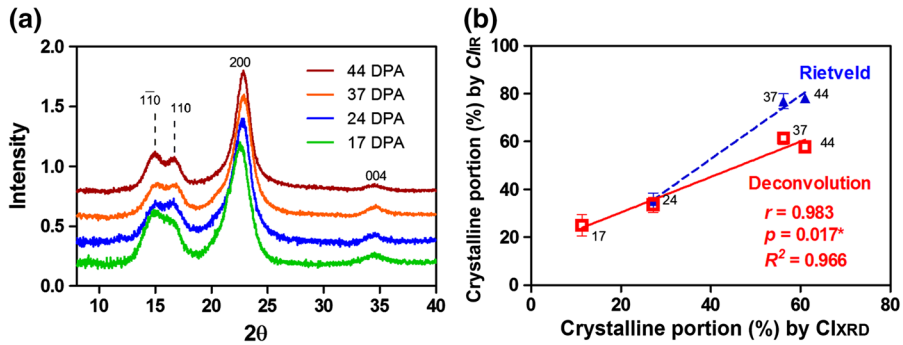

Fig. 6 Correlation of crystallinity index values of developing cotton fibers measured between FT-IR and XRD method. **a** X-ray diffractograms of *G. hirsutum* TM-1 fiber powders at 17, 24, 37, and 44 DPA. Linear backgrounds were subtracted from raw data. **b** The crystalline portions of total cellulose were calculated based on the XRD CI_{XRD} values determined by both deconvolution and Rietveld methods, and FT-IR CI_{IR} values determined by a simple algorithm from developing fibers

the three band algorithm (Table 3 and Fig. 6b). There were significant correlations ($R^2 = 0.968$; $p = 0.016$*) of the crystalline portions determined by the peak deconvolution method when they were calculated from the total cellulose contents of developing fibers. The results showed that the CI_{IR} values determined from FT-IR spectra could be used to calculate the crystalline portions that successfully trace the progress of SCW development during cotton fiber development, although they were not quantitatively matched to the CI_{XRD} values determined from XRD profiles.

Here, it should be noted that calculation of the CI_{XRD} values from XRD profiles is subject to the base line corrections and the XRD peaks can be affected in a complex manner with the crystalline component concentration and crystallite size (Lee et al. 2015a). For example, the (200) peak position of the 17 DPA XRD peak position is slightly lower in 2θ than those of the higher DPA samples (Fig. 6a), indicting the spacing between (200) crystallographic planes is slightly larger. This could be due to low degree of cellulose chain packing in the PCW development stage. For that reason, the Rietveld refining did not work well for the 17 DPA XRD data; thus, the CI_{XRD} of the 17 DPA sample could not be determined from the Rietveld method. However, the peak deconvolution method is not affected by any differences in the peak position because the peak deconvolution method simply ignores subtle deviations in the crystalline order. It is important to note that this does not mean the deconvolution method is better than the Rietveld method. Thus, the CI_{XRD} values must be considered as a qualitative or semi-quantitative evaluation of the

crystalline cellulose amounts of fiber samples (Lee et al. 2015a; Liu et al. 2012a).

It is also important to remember the different definition of crystallinity among Updegraff, IR, and XRD methods. The IR method is based on the absorption peaks sensitive to certain structural constraints imposed on the normal vibrational modes due to the crystalline lattice. Thus, it is the "crystallinity based on the vibrational mode difference". The Updegraff method is based on the difference in the hydrolysis rate between the crystalline and amorphous phases. Hence, it is the "crystallinity based on hydrolysis kinetics". The XRD method is based on scattering coherence of x-ray from planes with the same electron density. Therefore, it is the "crystallinity based on scattering coherence". The effects of amorphous phase in these three physical processes would not be the same. If the kinetics control is done properly in the Updegraff method and the peak selections as well as baseline corrections are done properly in the IR method, then these two methods can give "similar" values since both kinetics and IR are the linear sums. However, the XRD method involves many scattering processes including Bragg, thermal, Compton, etc., and the effects of the crystalline versus amorphous phases on the total signal in XRD vary among different scattering processes. Because of these differences in three methods, it may not be physically meaningful to come up with one common definition of "crystallinity". However, it would be still meaningful to compare the "crystallinity values" calculated from different methods and find which ones correlate better to one another since this allows researchers to use a simpler method to find the value equivalent to the more laborious method. For that reason, the crystallinity values estimated by the FT-IR spectroscopy from various plant tissues and textiles have been frequently compared with those determined by the XRD and other chemical methods (Abidi and Manike 2017; Åkerholm et al. 2004; Liu et al. 2012a; Nelson and O'Connor 1964; O'Connor et al. 1958; Oh et al. 2005; Schultz et al. 1985). Although we knew these limitations in CI_{XRD}, we compared the CI_{IR} values from the three band ratio algorithm with the CI_{XRD} values determined from the Rietveld and peak deconvolution methods because the CI_{XRD} values have been used so frequently and widely in the previous literature.

Comparison of SCW development in cultured fibers analyzed by FT-IR methods as well as chemical and genomic assays

We tested if and which FT-IR methods are sensitive enough to detect subtle differences of SCW cellulose biosynthesis that is regulated by phytohormones in culture conditions. For differentiating cotton fibers from unfertilized cotton ovules at DOA in vitro, a phytohormon, auxin, is required (Beasley and Ting 1974; Meinert and Delmer 1977). The SCW cellulose biosynthesis in cotton fibers cultured with a synthetic auxin, NAA, is delayed as compared with that in cotton fibers cultured with a natural auxin, IAA (Singh et al. 2009). Thus, we cultured DOA ovules with 5 μM IAA or 5 μM NAA for 13, 17, 24, and 27 DPA (Fig. 7a, b), and compared transcript abundance of *GhCesA2* responsible for SCW cellulose biosynthesis in cotton fibers. Comparisons of *GhCesA2* transcript levels by RT-qPCR showed a recognizable interval of *GhCesA2* expression responsible for SCW biosynthesis of cotton fibers when cotton ovules were cultured with IAA or NAA (Fig. 7c). IAA up-regulated *GhCesA2* transcript levels between 13 and 17 DPA, whereas NAA up-regulated *GhCesA2* transcript levels between 17 and 24 DPA. We previously showed that the onset of the *GhCesA2* up-regulation indicates a transition from PCW to SCW stage during cotton fiber development (Kim et al. 2012).

We further analyzed the developing fibers cultured with IAA or NAA by comparing cellulose contents (Fig. 8a), CI_{IR} values from the three FT-IR bands (Fig. 8b), and two different PCA methods with entire IR spectra (Fig. 8c) or cellulose IR spectral regions (Fig. 8d). Consistent with the *GhCesA2* transcript levels in Fig. 7c, the CI_{IR} and PC1 values of developing fibers cultured with IAA were higher than those cultured with NAA at three developmental time points. However, the patterns of increasing cellulose levels and CI_{IR} values from developing fibers cultured with IAA and NAA were substantially different from those of the PC1 scores from the same developing fibers.

The differences between cellulose levels and CI_{IR} values cultured between IAA and NAA significantly increased from 17 to 27 DPA and the greatest difference was found at 27 DPA (Fig. 8a, b). In contrast, the PC1 scores calculated from entire IR spectra (Fig. 8c) and the cellulose IR spectra (Fig. 8d)

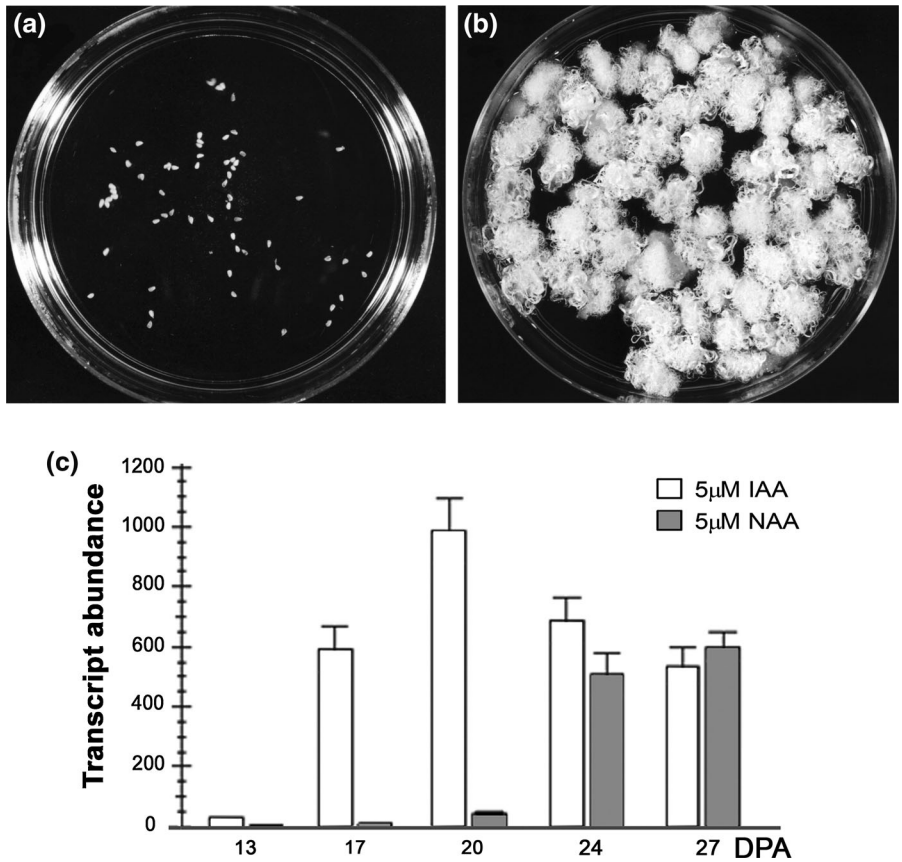

Fig. 7 Differential expressions of *GhCesA2* transcript responsible for SCW cellulose biosynthesis by two different phytohormones. **a** Unfertilized ovules at day of anthesis (DOA) in petri dish. **b** Cultured cotton ovules with developing fibers at 24 DPA. Unfertilized ovules at DOA were cultured on basal medium with a natural auxin and GA_3 for 24 days. **c** Comparisons of *GhCesA2* transcript abundance from developing fibers cultured with different phytohormones. Unfertilized cotton ovules at DOA were cultured with 0.5 μM GA_3 containing either a natural auxin (5 μM IAA) or a synthetic auxin (5 μM NAA) for 13, 17, 20, 24, and 27 DPA. *GhCesA2* transcript levels in developing fibers were determined RT-qPCR and normalized with 18S rRNA (U42827) and α-tubulin 4 (AF106570) as references genes

similarly increased from 17 to 24 DPA, but not from 24 to 27 DPA. Unlike the cellulose and CI_{IR} results (Fig. 8a, b), a very little difference was detected at the 27 DPA fibers cultured between IAA and NAA (Fig. 8c, d). With the FT-IR spectra obtained from the developing fibers at the active SCW stage (27 DPA) cultured with IAA or NAA, the two PCA methods failed to distinguish the different progress of SCW cellulose biosynthesis, although it successfully detected the differences during PCW and transition stage (Fig. 8c, d). These results were very similar to those in Figs. 3b and 4b, confirming that the PCA method was not sensitive enough to show the progress of SCW development from both field grown and cultured fibers. Therefore, we concluded the CI_{IR} values determined from the FT-IR enabled the progressive quantitative measurement in cellulose content, whereas the PCA methods with the entire spectra or cellulose spectral regions were only able to differentiate SCW from PCW.

Comparison of SCW development in different cotton species between FT-IR and chemical assays

We also tested whether any FT-IR methods enabled the monitoring of differences in fiber SCW development between two cotton species. *G. arboreum* is the closest diploid cotton species (A_2 genome) of the maternal parent for the allotetraploid cotton species, *G. hirsutum* (AD_1 genome) that is the agriculturally

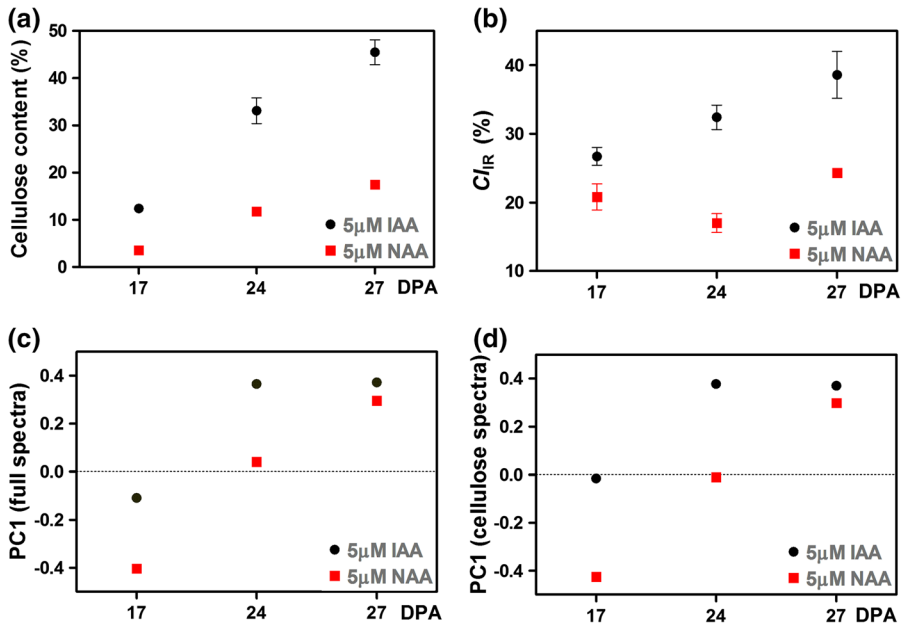

Fig. 8 Comparisons of methods of detecting cellulose biosynthesis that is differentially regulated by various phytohomones during cotton fiber development. Unfertilized cotton ovules at DOA were cultured in vitro with 0.5 μM GA_3 containing either a natural auxin (5 μM IAA) or a synthetic auxin (5 μM NAA) for 13, 17, 20, 24, and 27 DPA. Comparisons of cellulose contents (**a**), crystallinity index, CI_{IR} % (**b**), PC1 scores of full IR spectra (**c**), and PC1 scores of cellulose IR spectra (**d**) in developing *G. hirsutum* TM-1 fibers at various DPA cultured with IAA or NAA

important cotton species (Applequist et al. 2001; Wendel and Cronn 2003). The diploid A_2 cotton genome was sequenced from *G. arboretum* SXY1 (Li et al. 2014), and the allotetraploid AD_1 genome was sequenced from *G. hirsutum* TM-1 (Li et al. 2015; Zhang et al. 2015). Different fiber lengths between the two species were visually detected (Fig. 9a). *G. arboreum* SXY1 undergoes an earlier transition to SCW stage as compared to *G. hirsutum* TM-1 (Li et al. 2015).

Cellulose levels (Fig. 9b) of both cotton species were low at the PCW stage (12 DPA). At the early SCW stage (23 DPA), cellulose content of *G. arboreum* SXY1 fibers (62.8%) was significantly higher than that of *G. hirsutum* TM-1 fibers (44.3%) as predicted by Li et al. (2015). During the SCW stage from 23 to 30 DPA, the cellulose contents of both *G. arboreum* (89.9%) and *G. hirsutum* (87.2%) significantly increased and became similar to each other. We also measured CI_{IR} values from the three IR bands (Fig. 9c), PC1 scores from entire IR spectra (Fig. 9d), and PC1 scores from cellulose IR regions (Fig. 9e) of the two cotton species. Both species showed low PC1 scores and CI_{IR} % commonly at PCW stage (12 DPA). At the early SCW stage (23 DPA), the CI_{IR} values (Fig. 9c) showed significant differences between *G. arboreum* and *G. hirsutum* that were consistently monitored by the cellulose assay (Fig. 9b), whereas both PC1 scores commonly failed to show differences (Fig. 9d, e).

During the active SCW stage from 23 to 30 DPA, the CI_{IR} values continued to increase as the cellulose contents increased, whereas the both PC1 scores had not changed. As results, we concluded that the algorithm with three bands was able to trace the SCW developments from two different cotton species as the reference chemical method did, whereas the PCA method with entire spectral and cellulose regions proved insufficient when attempting to determine the degree of SCW biosynthesis.

Conclusion

We compared three different FT-IR methods to identify which method can estimate SCW cellulose level from cotton fibers in a quantitative way. The two methods analyzing the entire spectra and cellulose

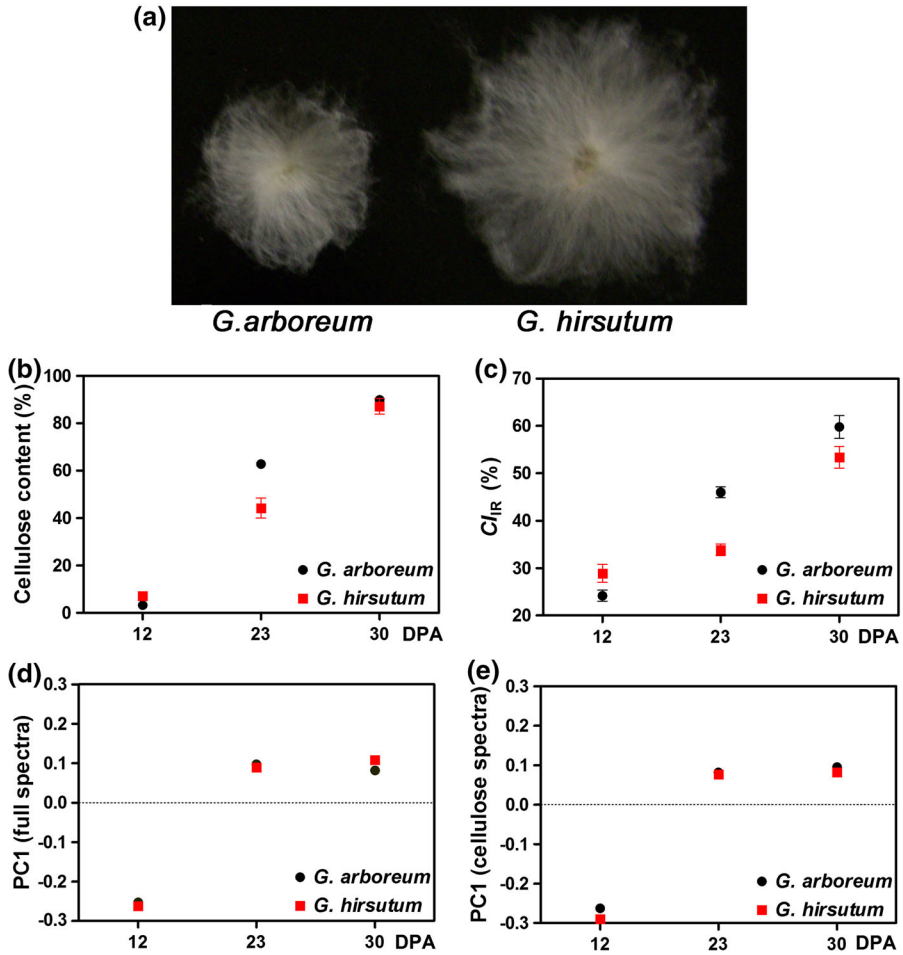

Fig. 9 Comparisons of methods of monitoring cellulose biosynthesis between two different cotton species. **a** Cottonseed phenotype between *G. arboreum* SXY1 and *G. hirsutum* TM-1. **b–e** Comparisons of fiber properties measured by different methods. cellulose contents (**b**), crystallinity index CI_{IR} % (**c**), PC1 scores of full IR spectra (**d**), and PC1 scores of cellulose IR spectra (**e**) were determined from developing fibers at 12, 23, and 30 DPA between *G. arboreum* SXY1 and *G. hirsutum* TM-1

regions by PCA showed a transition from the PCW to the SCW biosynthesis stage, but they cannot quantitatively determine SCW levels. In contrast, the CI_{IR} values determined from three FT-IR bands quantitatively monitor cotton fiber development including both PCW and SCW stage. Thus, the FT-IR method that can measure SCW cellulose in a quantitative, quick, and non-invasive way from a very small amount of cotton fibers may improve the way of phenotyping cotton fibers, interpreting genomic data, and identifying the molecular mechanisms of SCW cellulose depositions that affect cotton fiber properties and quality.

Acknowledgments This research was supported by the USDA-ARS Research Project #6054-21000-017-00D, and Cotton Incorporated-Sponsored Project #12-199. Authors thank Drs. Zhongqi He and Huai Cheng of USDA-ARS, Southern Regional Research Center for critically reviewing the manuscript. Authors acknowledge Ms. Tracy Condon for fiber sample preparation, and Mr. Wilson Buttram and Keith Stevenson for preparing cotton fields. Mention of trade names or commercial products in this article is solely for the purpose of providing specific information and does not imply recommendation or endorsement by the U.S. Department of Agriculture which is an equal opportunity provider and employer.

References

Abidi N, Manike M (2017) X-ray diffraction and FTIR investigations of cellulose deposition during cotton fiber development. Text Res J 0040517516688634

Abidi N, Hequet E, Cabrales L, Gannaway J, Wilkins T, Wells LW (2008) Evaluating cell wall structure and composition of developing cotton fibers using Fourier transform infrared spectroscopy and thermogravimetric analysis. J Appl Polym Sci 107:476–486

Abidi N, Cabrales L, Hequet E (2010a) Fourier transform infrared spectroscopic approach to the study of the secondary cell wall development in cotton fiber. Cellulose 17:309–320

Abidi N, Hequet E, Cabrales L (2010b) Changes in sugar composition and cellulose content during the secondary cell wall biogenesis in cotton fibers. Cellulose 17:153–160

Abidi N, Cabrales L, Haigler CH (2014) Changes in the cell wall and cellulose content of developing cotton fibers investigated by FTIR spectroscopy. Carbohydr Polym 100:9–16

Åkerholm M, Hinterstoisser B, Salmén L (2004) Characterization of the crystalline structure of cellulose using static and dynamic FT-IR spectroscopy. Carbohydr Res 339:569–578

Applequist WL, Cronn R, Wendel JF (2001) Comparative development of fiber in wild and cultivated cotton. Evol Dev 3:3–17

Beasley C, Ting IP (1974) Effects of plant growth substances on in vitro fiber development from unfertilized cotton ovules. Am J Bot 61:188–194

Brims M, Hwang H (2010) Introducing Cottonscope: a rapid and precise measurement of cotton fibre maturity based on siromat. National Cotton Council, New Orleans

Brown DM (2005) Identification of novel genes in Arabidopsis involved in secondary cell wall formation using expression profiling and reverse genetics. Plant Cell 17:2281–2295. https://doi.org/10.1105/tpc.105.031542

Chen L, Carpita NC, Reiter WD, Wilson RH, Jeffries C, McCann MC (1998) A rapid method to screen for cell-wall mutants using discriminant analysis of Fourier transform infrared spectra. Plant J 16:385–392

Driemeier C, Calligaris GA (2011) Theoretical and experimental developments for accurate determination of crystallinity of cellulose I materials. J Appl Crystallogr 44:184–192

Fang L, Tian R, Li X, Chen J, Wang S, Wang P, Zhang T (2014) Cotton fiber elongation network revealed by expression profiling of longer fiber lines introgressed with different *Gossypium barbadense* chromosome segments. BMC Genomics 15:838

French AD, Santiago Cintrón M (2013) Cellulose polymorphy, crystallite size, and the Segal crystallinity index. Cellulose 20:583–588

Gordon S, Rodgers J (2017) Cotton fibre cross-section properties. In: Gordon S, Abidi N (eds) Cotton fibres, characteristics, uses and performance. Nova Science Publishers, Inc., New York, pp 65–86

Haigler C (2010) Physiological and anatomical factors determining fiber structure and utility. In: Stewart JM, Oosterhuis DM, Heitholt JJ, Mauney JR (eds) Physiology of cotton. Springer, New York, pp 33–47

Hsieh Y-L (1999) Structural development of cotton fibers and linkages to fiber quality. In: Basra AS (ed) Cotton fibers developmental biology, quality improvement, and textile processing. Haworth Press, Inc., New York, pp 137–165

Imai T, Sugiyama J (1998) Nanodomains of Iα and Iβ cellulose in algal microfibrils. Macromolecules 31:6275–6279

Kemsley EK (1998) Discriminant analysis and class modelling of spectroscopic data. Wiley, Chichester

Kim HJ (2015) Fiber biology. In: Fang DD, Percy RG (eds) Cotton, 2nd edn. Agronomy monograph. American Society of Agronomy, Crop Science Society of America, and Soil Science Society of America, Madison, WI, pp 97–127

Kim HJ, Triplett BA (2001) Cotton fiber growth in planta and in vitro. Models for plant cell elongation and cell wall biogenesis. Plant Physiol 127:1361–1366

Kim HJ, Triplett BA, Zhang H-B, Lee M-K, Hinchliffe DJ, Li P, Fang DD (2012) Cloning and characterization of homeologous cellulose synthase catalytic subunit 2 genes from allotetraploid cotton (*Gossypium hirsutum* L.). Gene 494:181–189

Kim HJ, Tang Y, Moon HS, Delhom CD, Fang DD (2013a) Functional analyses of cotton (*Gossypium hirsutum* L.) immature fiber (im) mutant infer that fiber cell wall development is associated with stress responses. BMC Genomics 14:889

Kim SH, Lee CM, Kafle K (2013b) Characterization of crystalline cellulose in biomass: basic principles, applications, and limitations of XRD, NMR, IR, Raman, and SFG. Korean J Chem Eng 30:2127–2141

Kim HJ, Rodgers J, Delhom C, Cui X (2014) Comparisons of methods measuring fiber maturity and fineness of Upland cotton fibers containing different degree of fiber cell wall development. Text Res J 84:1622–1633

Kim HJ et al (2017) Comparative physical and chemical analyses of cotton fibers from two near isogenic upland lines differing in fiber wall thickness. Cellulose 24:2385–2401

Kohel R, Richmond T, Lewis C (1970) Texas marker-1. Description of a genetic standard for *Gossypium hirsutum* L. Crop Sci 10:670–671

Langan P, Nishiyama Y, Chanzy H (2001) X-ray structure of mercerized cellulose II at 1 Å resolution. Biomacromolecules 2:410–416

Lee CM, Dazen K, Kafle K, Moore A, Johnson DK, Park S, Kim SH (2015a) Correlations of apparent cellulose crystallinity determined by XRD, NMR, IR, Raman, and SFG methods. In: Rojas OJ (ed) Cellulose chemistry and properties: fibers, nanocelluloses and advanced materials. Advances in polymer science. Springer, Cham, pp 115–131

Lee CM, Kafle K, Belias DW, Park YB, Glick RE, Haigler CH, Kim SH (2015b) Comprehensive analysis of cellulose content, crystallinity, and lateral packing in *Gossypium hirsutum* and *Gossypium barbadense* cotton fibers using sum frequency generation, infrared and Raman spectroscopy, and X-ray diffraction. Cellulose 22:971–989

Li F et al (2014) Genome sequence of the cultivated cotton *Gossypium arboreum*. Nat Genet 46:567–572

Li F et al (2015) Genome sequence of cultivated Upland cotton (*Gossypium hirsutum* TM-1) provides insights into genome evolution. Nat Biotechnol 33:524–530

Liu Y, Kim HJ (2015) Use of Attenuated Total Reflection Fourier Transform Infared (ATR FT-IR) spectroscopy in

direct, non-destructive, and rapid assessment of developmental cotton fibers grown in planta and in culture. Appl Spectrosc 69:1004–1010

Liu Y, Thibodeaux D, Gamble G (2011) Development of Fourier transform infrared spectroscopy in direct, non-destructive, and rapid determination of cotton fiber maturity. Text Res J 81:1559–1567

Liu Y, Thibodeaux D, Gamble G, Bauer P, VanDerveer D (2012a) Comparative investigation of Fourier transform infrared (FT-IR) spectroscopy and X-ray diffraction (XRD) in the determination of cotton fiber crystallinity. Appl Spectrosc 66:983–986

Liu Y, Thibodeaux D, Gamble G, Bauer PJ, Van Derveer D (2012b) FT-MID-IR spectroscopic investigation of fiber maturity and crystallinity at single boll level and a comparison with XRD approach. In: Beltwide Cotton Conference, Orlando, FL. National Cotton Council, pp 1213–1222

Long RL, Bange MP, Gordon SG, Constable GA (2010) Measuring the maturity of developing cotton fibers using an automated polarized light microscopy technique. Text Res J 80:463–471

Lutterotti L (2010) Total pattern fitting for the combined size–strain–stress–texture determination in thin film diffraction. Nucl Instrum Methods Phys Res Sect B 268:334–340

McCann MC, Hammouri M, Wilson R, Belton P, Roberts K (1992) Fourier transform infrared microspectroscopy is a new way to look at plant cell walls. Plant Physiol 100:1940–1947

McCann MC et al (2001) Approaches to understanding the functional architecture of the plant cell wall. Phytochemistry 57:811–821

Meinert MC, Delmer DP (1977) Changes in biochemical composition of the cell wall of the cotton fiber during development. Plant Physiol 59:1088–1097

Mouille G, Robin S, Lecomte M, Pagant S, Höfte H (2003) Classification and identification of Arabidopsis cell wall mutants using Fourier-Transform InfraRed (FT-IR) microspectroscopy. Plant J 35:393–404

Nam S, French AD, Condon BD, Concha M (2016) Segal crystallinity index revisited by the simulation of X-ray diffraction patterns of cotton cellulose Iβ and cellulose II. Carbohydr Polym 135:1–9

Nelson ML, O'Connor RT (1964) Relation of certain infrared bands to cellulose crystallinity and crystal lattice type. Part II. A new infrared ratio for estimation of crystallinity in celluloses I and II. J Appl Polym Sci 8:1325–1341

Nishiyama Y, Langan P, Chanzy H (2002) Crystal structure and hydrogen-bonding system in cellulose Iβ from synchrotron X-ray and neutron fiber diffraction. J Am Chem Soc 124:9074–9082

O'Connor RT, DuPré EF, Mitcham D (1958) Applications of infrared absorption spectroscopy to investigations of cotton and modified cottons: part I: physical and crystalline modifications and oxidation. Text Res J 28:382–392

Oh SY et al (2005) Crystalline structure analysis of cellulose treated with sodium hydroxide and carbon dioxide by means of X-ray diffraction and FTIR spectroscopy. Carbohydr Res 340:2376–2391

Park S, Baker JO, Himmel ME, Parilla PA, Johnson DK (2010) Cellulose crystallinity index: measurement techniques and their impact on interpreting cellulase performance. Biotechnol Biofuels 3:1

Paudel D, Hequet E, Noureddine A (2013) Evaluation of cotton fiber maturity measurements. Ind Crops Prod 45:435–441

Rodgers J, Delhom C, Hinchliffe D, Kim HJ, Cui X (2013) A rapid measurement for cotton breeders of maturity and fineness from developing and mature fibers. Text Res J 83:1439–1451

Sassi J-F, Tekely P, Chanzy H (2000) Relative susceptibility of the Iα and Iβ phases of cellulose towards acetylation. Cellulose 7:119–132

Schultz T, McGinnis G, Bertran M (1985) Estimation of cellulose crystallinity using fourier transform-infrared spectroscopy and dynamic thermogravimetry. J Wood Chem Technol 5:543–557

Segal L, Creely J, Martin A Jr, Conrad C (1959) An empirical method for estimating the degree of crystallinity of native cellulose using the X-ray diffractometer. Text Res J 29:786–794

Singh B, Cheek HD, Haigler CH (2009) A synthetic auxin (NAA) suppresses secondary wall cellulose synthesis and enhances elongation in cultured cotton fiber. Plant Cell Rep 28:1023–1032. https://doi.org/10.1007/s00299-009-0714-2

Updegraff DM (1969) Semimicro determination of cellulose in biological materials. Anal Biochem 32:420–424

Vorwerk S, Somerville S, Somerville C (2004) The role of plant cell wall polysaccharide composition in disease resistance. Trends Plant Sci 9:203–209

Wakelyn PJ et al (2010) Cotton fiber chemistry and technology, vol 17. International fiber science and technology series. CRC Press, New York

Wang C, Lv Y, Xu W, Zhang T, Guo W (2014) Aberrant phenotype and transcriptome expression during fiber cell wall thickening caused by the mutation of the Im gene in immature fiber (im) mutant in *Gossypium hirsutum* L. BMC Genomics 15:94

Wendel JF, Cronn RC (2003) Polyploidy and the evolutionary history of cotton. Adv Agron 78:139–186

Yamamoto H, Horii F, Hirai A (1996) In situ crystallization of bacterial cellulose II. Influences of different polymeric additives on the formation of celluloses I α and I β at the early stage of incubation. Cellulose 3:229–242

Zhang T et al (2015) Sequencing of allotetraploid cotton (*Gossypium hirsutum* L. acc. TM-1) provides a resource for fiber improvement. Nat Biotechnol 33:531–537